Article

Not peer-reviewed version

Effect of Complexation with Closo-Decaborate Anion on Photophysical Properties of Copolyfluorenes Containing Dicyanophenanthrene Units in the Main Chain

Anton A. Yakimanskiy , Ksenia I. Kaskevich , Tatiana G. Chulkova , Elena L. Krasnopeeva * , Vera V. Voinova , Nikolay K. Neumolotov , Andrey P. Zhdanov , Konstantin Yu. Zhizhin , Anastasia V. Rogova , Felix N. Tomilin , Alexander V. Yakimansky

Posted Date: 19 October 2023

doi: 10.20944/preprints202310.1206.v1

Keywords: copolyfluorene; nitrilium derivatives of closo-decaborate anions; luminescence; phenanthrene-9,10-dicarbonitrile

Article

Effect of Complexation with Closo-Decaborate Anion on Photophysical Properties of Copolyfluorenes Containing Dicyanophenanthrene Units in the Main Chain

Anton A. Yakimanskiy [1], Ksenia I. Kaskevich [1], Tatiana G. Chulkova [1], Elena L. Krasnopeeva [1,*], Serguei V. Savilov [2,3], Vera V. Voinova [3], Nikolay K. Neumolotov [3], Andrey P. Zhdanov [3], Anastasia V. Rogova [4], Felix N. Tomilin [4,5], Konstantin Yu. Zhizhin [3] and Alexander V. Yakimansky [1]

[1] Institute of Macromolecular Compounds RAS, Bolshoi Prospect of Vasilyevsky Island 31, St. Petersburg, 199004, Russia; yakimanskii@gmail.com (A.A.Y.); kaskevich-ksenia@yandex.ru (K.I.K.); tgc@mail.ru (T.G.C.); yakimansky@yahoo.com (A.V.Y.)

[2] Department of Chemistry, Lomonosov Moscow State University, Moscow, 119991, Russia; savilov@mail.ru

[3] Kurnakov Institute of General and Inorganic Chemistry RAS, Moscow, 119991, Russia; savilov@mail.ru (S.V.S); veravoinova@rx24.ru (V.V.V.); neumolotovn@gmail.com (N.K.N.); zh_dots@mail.ru (A.P.Z.); zhizhin@igic.ras.ru (K.Y.Z.)

[4] Kirensky Institute of Physics, Federal Research Center KSC SB RAS, Krasnoyarsk, 660036, Russia; arogova1927@gmail.com (A.V.R.); felixnt@gmail.com (F.N.T.)

[5] Laboratory for Digital Controlled Drugs and Theranostics, Federal Research Center "Krasnoyarsk Science Center SB RAS", Krasnoyarsk, 660041, Russia; felixnt@gmail.com

* Correspondence: opeeva@gmail.com; Tel.: +7-812-3237407

Abstract: The functionalization of copolyfluorenes containing dicyanophenanthrene units by *closo*-decaborate anion is described. Target copolyfluorenes were analyzed using SEM, UV-vis, luminescence, NMR and Fourier-transform infrared (FTIR) spectroscopy. The effect of complexation with the *closo*-decaborate anion on the photophysical properties was studied both experimentally and theoretically. The PL data indicate an efficient charge transfer from fluorene to the dicyanophenanthrene units coordinated to *closo*-decaborate. The coordination of *closo*-decaborate clusters to the nitrile groups of copolyfluorenes provides an important route to new materials for sensors and light-emitting devices while at the same time serving as a platform for further study of the nature of boron clusters.

Keywords: copolyfluorene; nitrilium derivatives of *closo*-decaborate anions; luminescence; phenanthrene-9,10-dicarbonitrile

1. Introduction

Copolyfluorenes (CPFs) are very important for the practical advanced applications of optoelectronic and photovoltaic devices as well as biomedicine due to their luminescence and charge mobility properties. The donor-acceptor architecture of CPFs with π-conjugated units (D–π–A copolymers) have attracted much attention owing to charge (CT) and energy transfer (ET) effects [1–5]. This strategy has been widely applied to design high-efficiency light-emitting polymers. In the donor-acceptor copolymer system, the proper electron-deficient group in addition to the electron-rich fluorene unit is a critical factor for obtaining excellent copolymer performance. The electron-deficient cyano substituted aromatic groups are effective and widely used acceptors as they provide excellent electron injection/transport, high photoluminescence, as well as thermal stability. Measures such as incorporating an electron transport unit into the main chain were taken to balance the carrier transport to improve the EL performance. The coordination of boron cluster anions to nitriles leads to an increase in the electrophilicity of the carbon atom of the cyano group. As a result, the boron

 doi:10.20944/preprints202310.1206.v1

clusters can affect the electron-withdrawing properties of coordinated cyano groups as well as the luminescence of functionalized copolyfluorenes with cyano-substituted units. CT and ET processes may have important impact on the performance of optoelectronic devices and therefore deserve careful study. The efficiencies of CT and ET depend very sensitively on the donor-acceptor distance, on the energy-level (or bands) offsets, and on the local dielectric and electrostatic environment. On the one hand, Förtser-type energy transfer, mediated by relatively long-range (up to several nm) dipole-dipole coupling, is now engineered in a variety of light-harvesting devices and distance sensors [6]. Charge transfer, on the other hand, is a much shorter-range process (about 1 nm) that plays a key role in a number of molecular and solid state systems and is at the origin of the operation of photodetectors and solar cells [7].

Based on the 9,10-dicyanophenanthrene electron-deficient acceptor together with the frequently used derivative of fluorene as donor (9,9-dioctylfluorene), a series of copolymers were synthesized and functionalized by *closo*-decaborate anion. *Closo*-decaborate functionalized copolyfluorenes with different content of 9,10-dicyanophenanthrene units were studied both photophysically and using theoretical calculations.

2. Materials and Methods

All reagents and starting materials were purchased from commercial suppliers and used without further purification. Solvents were purified by standard methods.

The polycondensation reactions were performed in the CEM Discover LabMate single-mode microwave reactor (CEM Corporation, Matthews, NC, USA) at a radiation frequency of 2.45 GHz and a maximum generator power of 300 W. The temperature of synthesis was controlled using an infrared sensor placed under the reaction vessel. The reaction parameters (temperature, power, time, stirring rate) were set manually.

Polymer films were prepared on an Ossila spin coater and dried or heated in a UT-4620 drying chamber. The CPF films were formed by spin coating on the glass from polymers solutions in toluene (200–220 μL). The toluene solution concentration was 10 mg/mL.

NMR spectra were recorded on a Bruker AVANCE–400 SB (400 MHz) spectrometer at room temperature. The UV-visible absorption spectra were recorded on a Shimadzu UV-1900 spectrophotometer. Photoluminescence spectra were measured using an RF-6000 spectrofluorophotometer. The absorption and emission spectra of the films were measured immediately before heating and then after exposure for 4 h in the drying chamber at 80 °C and a high ventilation mode. FT-IR spectra were recorded on a Shimadzu IR Affinity-1S spectrometer using a Quest single-reflection ATR accessory (Specac), KRS-5 prism, 7800–400 cm^{-1} range.

2.1. Synthesis of CPFs

CPFs containing 0.5, 2.5 and 5% of 9,10-dicyanophenanthrene units (PFCN0.5, PFCN2.5, and PFCN5, respectively) were synthesized via Suzuki–Miyaura cross-coupling reaction according to procedure described previously [8]. Their structures were confirmed by ^{1}H NMR and FT-IR spectroscopy. The molecular mass characteristics of copolyfluorenes are presented in the Supplementary Materials, Table S1.

2.2. Synthesis of CPFs derivatives of the closo-decaborate anion

Method A: PFCNx (30 mg for x = 0.5 or 20 mg for x = 2.5 and 5) and $(NBu_4)[B_{10}H_{11}]$ (1.1 eq. to the cyano groups containing in the copolymer, 0.4, 1.1 and 2.2 mg, respectively) were dissolved in 3 mL of anhydrous 1,2-dichloroethane and purged with argon for 15 min. The resulting solution was heated in the sealed tube for 6 h at 80 °C with stirring. The solution was dried on a rotary evaporator and the residual pale yellow solid stored in the drying chamber.

^{1}H NMR and FT-IR spectral data for the synthesized compounds (PFCN0.5+B, PFCN2.5+B, and PFCN5+B) are given in the Supplementary Materials, Table S2, Figure S1.

 doi:10.20944/preprints202310.1206.v1

Method B: PFCN2.5 (7 mg) and (Ph_4P)[$B_{10}H_{11}$] (5 mg, 10^{-2} mmol) were mixed, followed by the addition of 3 mL of dichloromethane. The reaction mixture was purged with argon and stirred in the sealed tube for 4 hours at 45 °C. Subsequently, the solvent was removed under reduced pressure on a rotary evaporator. The target product (PFCN2.5+B') was extracted with toluene, concentrated on a rotary evaporator, and dried under a vacuum.

^{1}H NMR, ^{11}B{^{1}H} NMR, and FT-IR spectra for PFCN2.5+B' are presented in the Supplementary Materials, Figures S2–S4.

2.3. Scanning Electron Microscopy (SEM)

The specimens were imaged by SEM using a JEOL JSM 6490 LV instrument. The energy of the primary electrons was 10 keV, the current was varied within the range of 2-40 pA. The focal length of the electron beam was varied in the range from 9 to 14 mm. The accelerating voltages were commonly set to 20 kV. The morphology of the samples was determined in the backscattered electron mode in low vacuum mode. For elemental microanalysis of the sample surface (EDS), an energy dispersive system EX-54 175 JMH (JEOL) was used. For the study, samples were placed on conductive tape and secured to the sample holder using it. To ensure electrical conductivity, a layer of gold was sputtered on top.

2.4. Calculation Methods

The atomic and electronic structure, electron density distribution, absorption and luminescence spectra, and oscillator strengths for the ionic forms of the phenanthrene molecules, including the solvent, were calculated using density functional theory (DFT). Calculations were performed for 3,6-di(4-methylphenyl)phenanthrene-9,10-dicarbonitrile coordinated to one (PFCN-B1, Figure 1a) or two *closo*-decaborate anion clusters $B_{10}H_9^-$ (PFCN-B2, Figure 1c,d). The SMD model [9] was used to account for the solvent (chloroform). All calculations were performed with the CAM-B3LYP functional [10]. It has been shown previously [8] that CAM-B3LYP better describes the phenanthrene molecule. To choose the most appropriate basis set, a comparative analysis of theoretically calculated spectra and experimental data was performed for each structure ($B_{10}H_9^-$, PFCN-B1, PFCN-B2). The 6-31+(p,d) basis was used for the *closo*-decaborate anion $B_{10}H_9^-$. The choice of basis was motivated by the fact that the $B_{10}H_9^-$ cluster is charged. For the calculation of the ionic forms of PFCN-B1 and PFCN-B2 the 6-31+(p,d) basis was chosen, which includes polarization and diffusion functions. Since further excited state geometries were calculated, the choice of the basis is an important step. In general, the SMD/CAM-B3LYP/6-31+(p,d) level of the DFT theory was preferred by the totality of the data. Absorption and luminescence spectra for all phenanthrene molecules (models) were obtained using TD theory [11]. The calculations were performed in the program GAMESS [12].

Preprints (www.preprints.org) | NOT PEER-REVIEWED | Posted: 19 October 2023 doi:10.20944/preprints202310.1206.v1

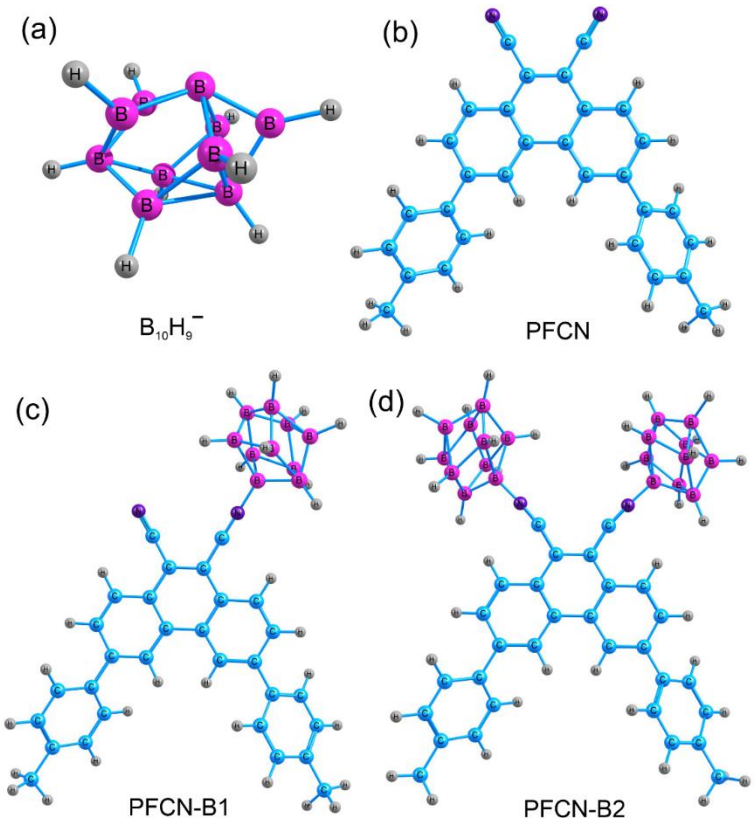

Figure 1. Atomic structures of the calculated molecules. (**a**) $B_{10}H_9^-$ anion cluster; (**b**) 3,6-di(4-methylphenyl)phenanthrene-9,10-dicarbonitrile (PFCN); (**c**) monofunctionalized 3,6-di(4-methylphenyl)phenanthrene-9,10-dicarbonitrile by closo-decaborate anion (PFCN-B1); (**d**) difunctionalized 3,6-di(4-methylphenyl)phenanthrene-9,10-dicarbonitrile by closo-decaborate anion (PFCN-B2). C, H, N, and B atoms are colored blue, gray, purple, and pink, respectively.

The calculations were performed as follows. (1) The $B_{10}H_9^-$ anion was constructed (Figure 1a). The geometry optimization in the ground and excited states was carried out in vacuum and taking into account the solvent (chloroform). The spectral properties of the cluster were then calculated. (2) Next, the effect of $B_{10}H_9^-$ on the phenanthrene molecule was investigated (Figure 1b). For this purpose, one or two nitrile groups of 3,6-di(4-methylphenyl)phenanthrene-9,10-dicarbonitrile were occupied by boron cluster anions (PFCN-B1 and PFCN-B2, Figure 1c,d). Geometry optimization in the ground and excited states was performed. A bsorption and luminescence spectra were calculated using TD/CAM-B3LYP level of theory.

The criterion for separating local transitions from charge transfer and Rydberg transitions is the analysis of the Λ parameter [10]. A value of $0.45 \leq \Lambda \leq 0.89$ indicates local excitations, which are characterized by a large overlap of molecular orbitals. In contrast, Rydberg transitions are characterized by a value in the range $0.08 \leq \Lambda \leq 0.27$, which is much smaller and indicates minimal spatial overlap between the occupied and virtual orbitals [10]. In calculations it was found that at absorption Λ parameter was in the range $0.14 < \Lambda < 0.41$, thus both local and charge transfer transitions are possible in these molecules.

3. Results and Discussion

3.1. Synthesis of closo-Decaborate Nitrilium Derivatives of CPFs with Dicyanophenanthrene units

Currently, the methods providing derivatives of the general formula $[B_{10}H_9NCR]^-$ with simple alkyl and aryl substituents have been reliably developed [13,14]. However, polymeric nitrilium derivatives with boron clusters have not yet been obtained. In this work, *closo*-decaborate nitrilium

Preprints (www.preprints.org) | NOT PEER-REVIEWED | Posted: 19 October 2023 doi:10.20944/preprints202310.1206.v1

derivatives of copolyfluorenes with 9,10-dicyanophenanthrene units (PFCNx+B) were synthesized according to the reaction scheme presented in Figure 2.

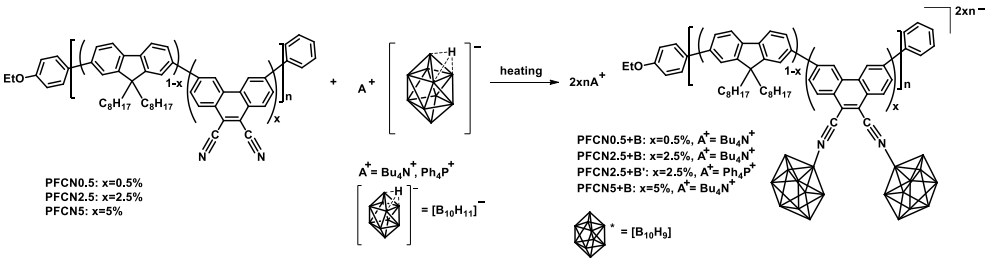

Figure 2. Synthesis of *closo*-decaborate nitrilium derivatives of copolyfluorenes with 9,10-dicyanophenanthrene units (PFCNx+B, PFCN2.5+B').

The reaction between the fluorene-based copolymer containing cyano groups and the *closo*-decaborate salt in its protonated form, $(Bu_4N)[B_{10}H_{11}]$ or $(Ph_4P)[B_{10}H_{11}]$, was conducted under conditions standard for the Electrophile-Induced Nucleophilic Substitution (EINS) mechanism [15]. An excess of *closo*-decaborate was used to make sure all the CN-groups in the copolymer are reacted. The reaction was monitored via ^{11}B, ^{1}H NMR spectroscopy, and IR spectroscopy. The most informative method was IR spectroscopy, which indicated the presence of B-H bonds in the reaction product (2400-2600 cm^{-1}) as well as CN-B (2350-2400 cm^{-1}) (Supplementary Materials, Table S2, Figure S4). These values are consistent with data obtained for the addition products of low molecular weight nitriles [16]. Due to the low concentration of cyano groups in the copolymer, NMR spectroscopy was less informative. In the ^{1}H NMR spectra of PFCNx+B, it is clearly seen the signals of tetrabutylammonium protons in the range from 1.0 to 3.3 ppm (Supplementary Materials, Table S2, Figure S1). In the ^{1}H NMR spectrum of PFCN2.5+B', the protons of the phenyl groups of the PPh_4^+ cation overlap with the aromatic protons of the copolymer in the region of 7.5–8.0 ppm. The protons associated with the boron atoms in the cluster appear in a broad range from 0 to 2 ppm and are not distinguishable due to the low concentration of the cluster in the substance and overlapping (Supplementary Materials, Figure S2). On the other hand, ^{11}B NMR provides with significant information. Although it seems hard to correlate signals with specific boron atoms, the overall spectrum shape qualitatively indicates the reaction progression. The absence of signals from the apical position of the original anion $[B_{10}H_{11}]^-$ at 26 ppm and the shift of signals from the backbone boron atoms to a higher field (Supplementary Materials, Figure S3) indicates two important things: (1) absence of the initial *closo*-decaborate in the system; (2) presence of a nitrile derivative of the *closo*-decaborate anion. The morphology of the as-prepared PFCN2.5+B' sample was analyzed by SEM (Figure 3). The sample has a layered structure with a particle size of 1-10 microns. Energy dispersive analysis data indicate the presence of phosphorus from the triphenylphosphonium cation (Supplementary Materials, Figure S5).

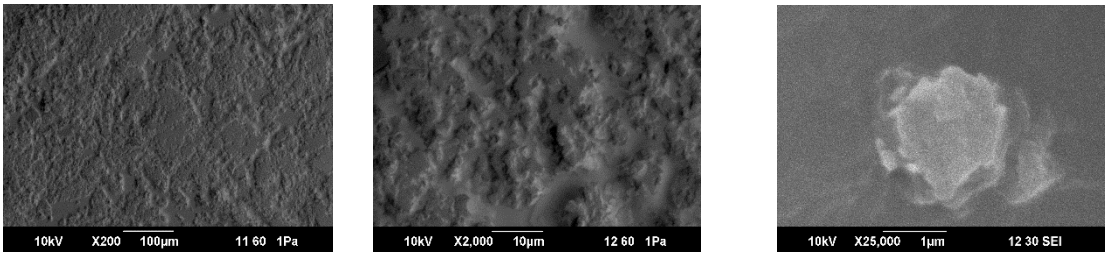

Figure 3. SEM images of PFCN2.5+B'.

The surface has a granular-fibrous morphology, typical for films of many polymers formed by the spin-coating method. At the same time, the sample contains grains (possibly also granules).

Preprints (www.preprints.org) | NOT PEER-REVIEWED | Posted: 19 October 2023 doi:10.20944/preprints202310.1206.v1

3.2. Photophysical Properties of Modified CPFs

The UV–vis absorption spectra of the PFCNx+B polymers were measured in films (Supplementary Materials, Table S3). The most intense band at ca. 385 nm in the spectra corresponds to the π–π* transition in the fluorene fragments [17–20].The same band is observed in the UV-vis spectra of the PFCNx polymers. In the polymer functionalized with boron clusters (PFCNx+B), the band at ca. 395 nm begins to appear. Also, the shoulder at ca. 430 nm becomes more intense and redshifted compared to the non-functionalized polymer.

In the photoluminescence spectra of the PFCNx+B films (Supplementary Materials, Table S3), the intensive band at 500–530 nm is observed. In general, the addition of boron clusters to the cyano groups of the copolymer leads to an increase in luminescence intensity (Supplementary Materials, Figure S6).

Probably, the observed Stokes shifts (Supplementary Materials, Table S3) are related to the degree of structural reorganization of the two-fold C_{2v}-symmetrical luminophoric dicyanophenanthrene moiety with boron clusters in the copolymers, intramolecular charge-transfer characteristics of the copolymers in the film state, or intermolecular charge-transfer between the *closo*-decaborate nitrilium units and fluorene moieties in the copolymers.

3.3. Theoretical Calculations

The absorption and emission maxima for PFCN-B1 and PFCN-B2 calculated by TD/SMD/CAM-B3LYP/6-31+(p,d) method are presented in Table 1. The calculation of the absorption spectra of the *closo*-decaborate cluster (the $S_0 \rightarrow S_2$ transition with an oscillator strength of 0.004 is 424 nm) shows that the *closo*-decaborate cluster can influence on the appearance of the shoulder in the experimental spectrum in the range of 425-450 nm (Supplementary Materials, Table S3). At the same time, the calculated oscillator strengths of the transitions in the emission spectra turned out to be low.

Table 1. Calculation of the spectral properties of PFCN-B1 and PFCN-B2 at the TD/SMD/CAM-B3LYP/6-31+(p,d) level of the theory.

Absorption			**Emission**		
Transition	λ, нм	*f*	Transition	λ, нм	*f*
PFCN-B1					
$S_0 \rightarrow S_1$	387	0.78	$S_5 \rightarrow S_0$	423	0.89
$S_0 \rightarrow S_2$	352	0.34	$S_4 \rightarrow S_0$	372	0.34
MO	HOMO	LUMO	$S_3 \rightarrow S_0$	347	0.11
E_{MO}	-6.33	-1.91	$S_2 \rightarrow S_0$	329	0.14
ΔE	4.42		$S_1 \rightarrow S_0$	318	0.26
PFCN-B2					
$S_0 \rightarrow S_1$	412	0.84	$S_4 \rightarrow S_0$	563	0.47
$S_0 \rightarrow S_2$	376	0.53	$S_3 \rightarrow S_0$	433	0.68
MO	HOMO	LUMO	$S_2 \rightarrow S_0$	396	0.27
E_{MO}	-6.04	-1.88	$S_1 \rightarrow S_0$	385	0.16
ΔE	4.16				

λ and f—maximum absorption wavelength (nm) and oscillator strength of the $S_0 \rightarrow S_i$ transitions; MO—molecular orbital; E_{MO}—energy of molecular orbitals, eV; ΔE—energy gap between HOMO and LUMO, eV.

Upon introduction of boron clusters ($B_{10}H_9$) into dicyanophenanthrene, an increase in light absorption intensity and splitting of one peak at 380 nm into two (at 380 nm and 397 nm) is experimentally observed. Two maximum absorption spectra at 387 nm and 352 nm are observed for compound PFCN-B1, while 412 nm and 376 nm are observed for PFCN-B2 (Table 1). The introduction of a cluster ($B_{10}H_9$) to the cyano group at the position 9 of phenanthrene shifts the theoretical maximum of the absorption spectrum to the red region (by 28 nm), while the introduction of the

Preprints (www.preprints.org) | NOT PEER-REVIEWED | Posted: 19 October 2023 doi:10.20944/preprints202310.1206.v1

second *closo*-decaborate cluster shifts it more to the long wavelength region (by 35 nm), relative to PFCN (phenanthrene without the boron cluster). Thus, there is a correspondence between the experimental values of the transition energies in the absorption spectrum and the energy corresponding to the position of the maximum of the calculated absorption spectrum for PFCN-B1 and PFCN-B2 (Figure 4).

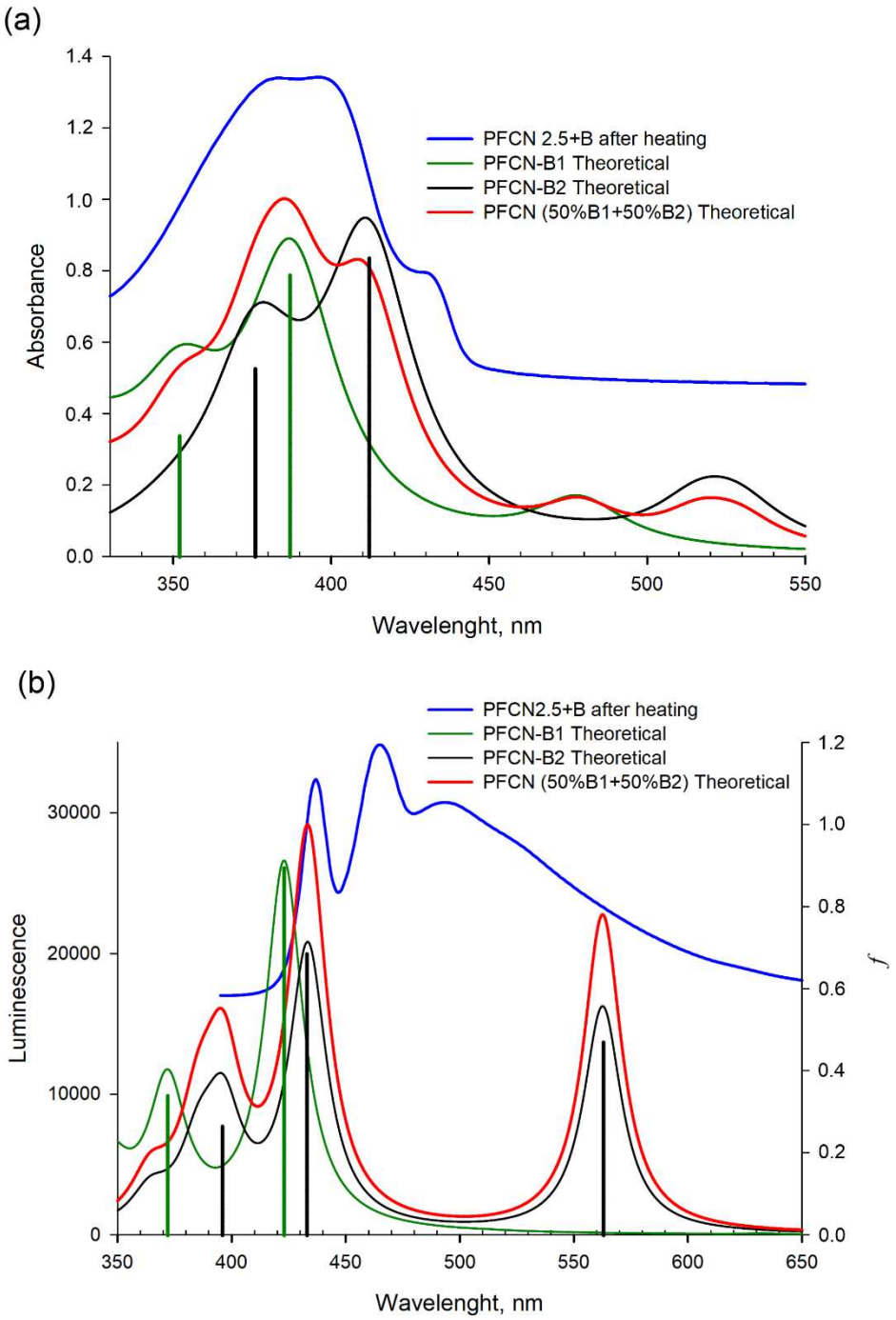

Figure 4. Experimental absorption and luminescence spectra and theoretical spectra for PFCN-B1 and PFCN-B2 structures calculated by TD/SMD/CAM-B3LYP/6-31+(p,d). (**a**)—Absorption spectrum. (**b**)—Luminescence spectrum. The experiment—blue line. Green vertical bar—theoretical electronic transition for PFCN-B1, green line—spectral model. Black vertical bar—theoretical electronic transition for PFCN-B2, black line—spectral model. Theoretical spectral model for a mixture of 50% PFCN-B1 and 50% PFCN-B2—red line.

Preprints (www.preprints.org) | NOT PEER-REVIEWED | Posted: 19 October 2023 doi:10.20944/preprints202310.1206.v1

A similar pattern is observed in the emission spectra. The addition of one boron cluster ($B_{10}H_9$) results in a shift (of 5 nm) to the red region (423 nm, Figure 4) relative to PFCN (417 nm [8]). The addition of the second boron cluster ($B_{10}H_9$) shifts the maximum of the emission spectrum to 433 nm and the additional peak appears in the red region (at 563 nm). Comparing the experimental and calculated data, a shift of the theoretical emission spectra to the blue region is observed relative to the experiment. Several emission bands are observed in the experimental luminescence spectrum, which may indicate that different parts of the molecule are independently involved in this process. In order to interpret this fact, a ten state TD/SMD/CAM-B3LYP/6-31+(pd) calculation was performed for the molecular geometry in the excited state (Supplementary Materials, Figures S7 and S8). As can be seen from these data, boron clusters are involved in the transitions visible in the emission spectra. The presence of a long-wavelength band in the experimental emission spectra indicates the addition of boron clusters to two cyano groups of the 9,10-dicyanophenanthrene fragment.

Figure S9 shows the ground state molecular structures and HOMO, LUMO orbitals for the PFCN-B1 (Supplementary Materials, Figure S9a,b) and PFCN-B2 (Supplementary Materials, Figure S9c,d) structures. The molecular orbitals show the groups of atoms involved in a particular transition, i.e., playing a key role in the absorption and excitation processes. As can be seen in Figure S9, for the PFCN-B1 structure, HOMOs are localized throughout the phenanthrene structure and cluster ($B_{10}H_9$). LUMO orbitals with electron density are already on phenanthrene-9,10-dicarbonitrile. A similar picture is observed for the PFCN-B2 structure.

All calculated structures show a slight difference in geometry with the addition of the boron cluster. The bond lengths and angles α1-3, β1-3, γ1-3, φ1-3 for PFCN, PFCN-B1 and PFCN-B2, respectively, were used to describe the change in the geometry of the molecules upon addition of the substituent $B_{10}H_9$ (Supplementary Materials, Figure S10a–f). When $B_{10}H_9$ is added, there is a change in the angle β1-3, when two $B_{10}H_9$ are added, the angles become less than 180°, but in the excited state, γ3, φ3 are closer to 180°. All this leads to the fact that the presence of two $B_{10}H_9$ must be accompanied by a bathochromic shift.

4. Conclusions

In summary, the first example of functionalization of CPFs containing 9,10-dicyanophenanthrene units by *closo*-decaborate anion was achieved. The reaction between the fluorene-based copolymer and *closo*-decaborate proceeds through the EINS mechanism.

The introduction of the $B_{10}H_9$ boron cluster affects the photophysical properties of copolyfluorenes. When the boron clusters are introduced into the dicyanophenanthrene unit, a splitting of one peak at 380 nm into two (at 380 nm and 397 nm) is experimentally observed. The PL emission spectra of the functionalized copolymers show significant energy transfer from fluorene segments to the dicyanophenanthrene units coordinated to the $B_{10}H_9$ boron clusters. These data are in good agreement with theoretical calculations. Our theoretical calculations show that the charge transfer takes place in the polymer chain from fluorene to the *closo*-decaborate nitrilium phenanthrene moieties.

Supplementary Materials: The following supporting information can be downloaded at the website of this paper posted on Preprints.org. Figure S1: ^{1}H NMR spectra of compounds (PFCN0.5+B, PFCN2.5+B, and PFCN5+B) in $CDCl_3$.; Figure S2: ^{1}H NMR spectrum of PFCN2.5+B′ in $CDCl_3$; Figure S3: $^{11}B\{^1H\}$ NMR spectrum of PFCN2.5+B′ in $CDCl_3$; Figure S4: FT-IR spectra of PFCN2.5 (top) and PFCN2.5+B′(bottom); Figure S5: EDS for PFCN2.5+B′; Figure S6: PL spectra of PFCN2.5, PFCN2.5+B, PFCN2.5 after heating at 80 °C for 4 h, and PFCN2.5+B after heating at 80 °C for 4 h in films; Figure S7: Transition scheme and molecular orbitals in the excited state of the PFCN-B1 molecule. Transition maxima in the luminescence spectrum according to Table 1. Energy of molecular orbitals in eV. The f is the oscillator strength. Maximum contributions of orbitals involved in this transition are given in percent (%). The inset shows the experimental luminescence spectrum; Figure S8: Transition scheme and molecular orbitals in the excited state of the PFCN-B2 molecule. Transition maxima in the luminescence spectrum according to Table 1. Energy of molecular orbitals in eV. The f is the oscillator strength. Maximum contributions of orbitals involved in this transition are given in percent (%). The inset shows the experimental luminescence spectrum; Figure S9: Molecular orbitals for the ground state of PFCN-B1 and PFCN-B2. a) Molecular orbitals for the $S_0 \rightarrow S_1$ transition of PFCN-B1; b) Molecular orbitals for the $S_0 \rightarrow S_2$

transition of PFCN-B1; c) Molecular orbitals for the $S_0 \rightarrow S_1$ transition of PFCN-B2; d) Molecular orbitals for the $S_0 \rightarrow S_2$ transition of PFCN-B2; Figure S10: Atomic structure of the calculated molecules in the ground and excited states. Bond lengths (Å) and angles characterizing the change in spatial structure upon introduction of the boron cluster ($B_{10}H_9^-$) in the ground and excited states for different phenanthrene compounds. a) PFCN geometry in the ground state; b) PFCN geometry in the excited state; c) PFCN-B1 geometry in the ground state; d) PFCN-B1 geometry in the excited state; e) PFCN-B2 geometry in the ground state; f) PFCN-B2 geometry in the excited state; Table S1: Molecular mass characteristics of copolyfluorenes; Table S2: FT-IR and ^{1}H NMR selected data for synthesized compounds; Table S3: UV-Vis and fluorescence spectral data for CPFs films.

Author Contributions: Conceptualization, A.P.Z., K.Y.Z., F.N.T., T.G.C., and A.V.Y.; Methodology, A.P.Z., F.N.T., T.G.C., S.V.S., and A.V.Y.; Formal analysis, A.P.Z., K.Y.Z., F.N.T., T.G.C., and A.V.Y.; Investigation, A.A.Y., K.I.K., V.V.V., N.K.N., A.V.R., S.V.S., and F.N.T.; Writing—original draft preparation, A.P.Z, T.G.C., F.N.T., S.V.S., and A.V.Y.; Writing—review and editing, T.G.C., E.L.K., K.Y.Z., F.N.T., and A.V.Y.; Supervision, T.G.C., A.P.Z., K.Y.Z., F.N.T., and A.V.Y.; project administration, T.G.C., E.L.K., and A.V.Y.; funding acquisition, A.V.Y.

Funding: This work was supported by the Russian Science Foundation, grant no. 23-43-00060.

Conflicts of Interest: The authors declare no conflict of interest.

References

1. Grimsdale, A.C.; Chan, K.L.; Martin, R.E.; Jokisz, P.G.; Holmes, A.B. Synthesis of Light-Emitting Conjugated Polymers for Applications in Electroluminescent Devices. *Chem. Rev.* **2009**, *109*, 897–1091, doi:10.1021/cr000013v.
2. Beaujuge, P.M.; Reynolds, J.R. Color Control in π-Conjugated Organic Polymers for Use in Electrochromic Devices. *Chem. Rev.* **2010**, *110*, 268–320.
3. Khasbaatar, A.; Xu, Z.; Lee, J.-H.; Campillo-Alvarado, G.; Hwang, C.; Onusaitis, B.N.; Diao, Y. From Solution to Thin Film: Molecular Assembly of π-Conjugated Systems and Impact on (Opto)Electronic Properties. *Chem. Rev.* **2023**, *123*, 8395–8487, doi:https://doi.org/10.1021/acs.chemrev.2c00905.
4. Kim, K.; Inagaki, Y.; Kanehashi, S.; Ogino, K. Synthesis of Polyfluorene-Polytriarylamine Block Copolymers with Light-Emitting Benzothiadiazole Moieties: Effect of Chromophore Location on Electroluminescent Properties. *Polym. J.* **2017**, *49*, 721–728, doi:10.1038/pj.2017.40.
5. Bezgin Carbas, B. Fluorene Based Electrochromic Conjugated Polymers: A Review. *Polymer (Guildf).* **2022**, *254*, 125040, doi:10.1016/j.polymer.2022.125040.
6. Guzelturk, B.; Demir, H.V. Near-Field Energy Transfer Using Nanoemitters For Optoelectronics. *Adv. Funct. Mater.* **2016**, *26*, 8158–8177, doi:10.1002/adfm.201603311.
7. May, V.; Kühn, O. *Charge and Energy Transfer Dynamics in Molecular Systems*; John Wiley & Sons, Inc.: New York, **2011**, 562.
8. Yakimanskiy, A.A.; Kaskevich, K.I.; Zhukova, E. V.; Berezin, I.A.; Litvinova, L.S.; Chulkova, T.G.; Lypenko, D.A.; Dmitriev, A. V.; Pozin, S.I.; Nekrasova, N. V.; et al. Synthesis, Photo- and Electroluminescence of New Polyfluorene Copolymers Containing Dicyanostilbene and 9,10-Dicyanophenanthrene in the Main Chain. *Materials (Basel).* **2023**, *16*, 1–15, doi:10.3390/ma16165592.
9. Tomasi, J.; Mennucci, B.; Cammi, R. Quantum Mechanical Continuum Solvation Models. *Chem. Rev.* **2005**, *105*, 2999–3093, doi:10.1021/cr9904009.
10. Peach, M.J.G.; Benfield, P.; Helgaker, T.; Tozer, D.J. Excitation Energies in Density Functional Theory: An Evaluation and a Diagnostic Test. *J. Chem. Phys.* **2008**, *128*, doi:10.1063/1.2831900.
11. Marques, M.A.L.; Gross, E.K.U. Time-Dependent Density Functional Theory. *Annu. Rev. Phys. Chem.* **2004**, *55*, 427–455, doi:10.1146/annurev.physchem.55.091602.094449.
12. Schmidt, M.W.; Baldridge, K.K.; Boatz, J.A.; Elbert, S.T.; Gordon, M.S.; Jensen, J.H.; Koseki, S.; Matsunaga, N.; Nguyen, K.A.; Su, S.; et al. General Atomic and Molecular Electronic Structure System. *J. Comput. Chem.* **1993**, *14*, 1347–1363, doi:10.1002/jcc.540141112.
13. Nelyubin, A. V.; Klyukin, I.N.; Zhdanov, A.P.; Grigor'ev, M.S.; Zhizhin, K.Y.; Kuznetsov, N.T. Synthesis of Nitrile Derivatives of the Closo-Decaborate and Closo-Dodecaborate Anions [BnHn – 1NCR]– (n = 10, 12) by a Microwave Method. *Russ. J. Inorg. Chem.* **2021**, *66*, 139–145, doi:10.1134/S0036023621020133.
14. Stogniy, M.Y.; Erokhina, S.A.; Sivaev, I.B.; Bregadze, V.I. Nitrilium Derivatives of Polyhedral Boron Compounds (Boranes, Carboranes, Metallocarboranes): Synthesis and Reactivity. *Phosphorus, Sulfur Silicon Relat. Elem.* **2019**, *194*, 983–988, doi:10.1080/10426507.2019.1631312.

15. Frank, R.; Adhikari, A.K.; Auer, H.; Hey-Hawkins, E. Electrophile-Induced Nucleophilic Substitution of the Nido- Dicarbaundecaborate Anion Nido-7,8-C2b9h12 by Conjugated Heterodienes. *Chem. - A Eur. J.* **2014**, *20*, 1440–1446, doi:10.1002/chem.201303762.
16. Ezhov, A. V.; Vyal'ba, F.Y.; Kluykin, I.N.; Zhdanova, K.A.; Bragina, N.A.; Zhdanov, A.P.; Zhizhin, K.Y.; Mironov, A.F.; Kuznetsov, N.T. Synthesis of New Bioinorganic Systems Based on Nitrilium Derivatives of Closo-Decaborate Anion and Meso-Arylporphyrins with Pendant Amino Groups. *Macroheterocycles* **2017**, *10*, 505–509, doi:10.6060/mhc171254z.
17. Klärner, G.; Lee, J.I.; Davey, M.H.; Miller, R.D. Exciton Migration and Trapping in Copolymers Based on Dialkylfluorenes. *Adv. Mater.* **1999**, *11*, 115–119, doi:10.1002/(SICI)1521-4095(199902)11:2<115::AID-ADMA115>3.0.CO;2-N.
18. Zhang, Q.; Chi, L.; Hai, G.; Fang, Y.; Li, X.; Xia, R.; Huang, W.; Gu, E. An Easy Approach to Control β-Phase Formation in PFO Films for Optimized Emission Properties. *Molecules* **2017**, *22*, 1–8, doi:10.3390/molecules22020315.
19. Zhao, S.; Liang, J.; Guo, T.; Wang, Y.; Chen, X.; Fu, D.; Xiong, J.; Ying, L.; Yang, W.; Peng, J.; et al. Formation of Poly(9,9-Dioctylfluorene) β-Phase by Incorporating Aromatic Moiety in Side Chain. *Org. Electron.* **2016**, *38*, 130–138, doi:10.1016/j.orgel.2016.08.007.
20. Perevedentsev, A.; Chander, N.; Kim, J.S.; Bradley, D.D.C. Spectroscopic Properties of Poly(9,9-Dioctylfluorene) Thin Films Possessing Varied Fractions of β-Phase Chain Segments: Enhanced Photoluminescence Efficiency via Conformation Structuring. *J. Polym. Sci. Part B Polym. Phys.* **2016**, *54*, 1995–2006, doi:10.1002/polb.24106.